AD-A114 674 ROYAL AIRCRAFT ESTABLISHMENT FARNBOROUGH (ENGLAND) F/G 20/4
THE ATTACHED FLOW OVER A SLENDER DELTA WING WITH LEADING-EDGE F--ETC(U)
JAN 82 A J PEACE
UNCLASSIFIED RAE/TR-81150 DRIC-BR-82792 NL

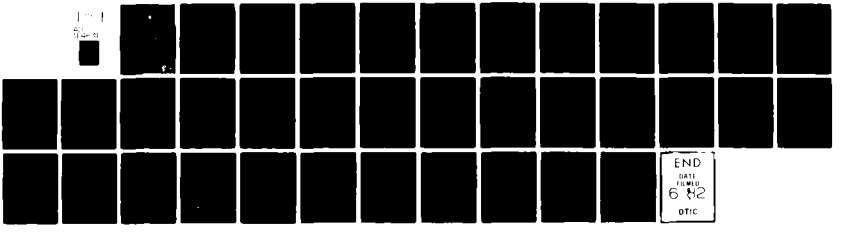

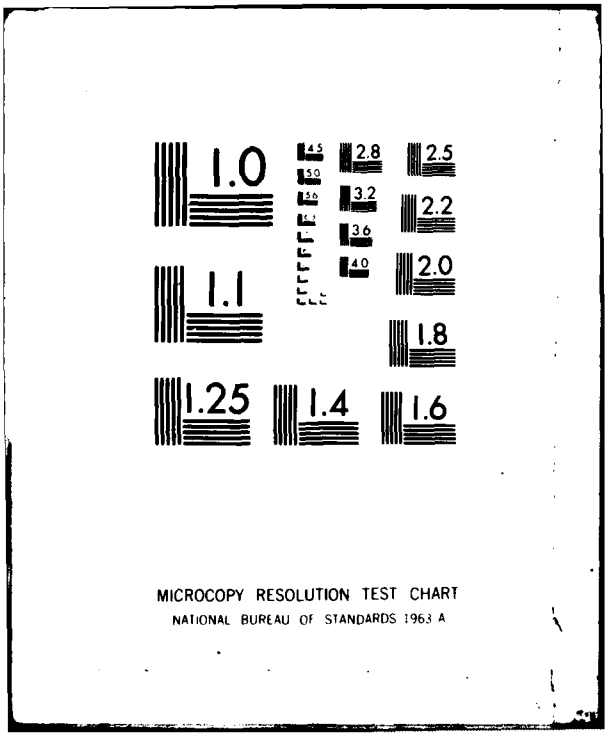
1.0
1.1
1.25
1.4
1.6
2.8
3.2
3.6
4.0
2.5
2.2
2.0
1.8
MICROCOPY RESOLUTION TEST CHART
NATIONAL BUREAU OF STANDARDS 1963 A

BR82792

TR 81150

AD A114674

ROYAL AIRCRAFT ESTABLISHMENT

*

Technical Report 81150

January 1982

THE ATTACHED FLOW OVER A SLENDER DELTA WING WITH LEADING-EDGE FLAPS

by

A. J. Peace

*

Procurement Executive, Ministry of Defence
Farnborough, Hants

82 05 17 111

UDC 533.693.3 : 533.696.7 : 533.694.25 : 533.6.011

ROYAL AIRCRAFT ESTABLISHMENT

Technical Report 81150

Received for printing 4 January 1982

THE ATTACHED FLOW OVER A SLENDER DELTA WING WITH LEADING-EDGE FLAPS

by

A. J. Peace*

SUMMARY

The flow over a delta wing with leading-edge flaps is considered within the framework of slender-body theory. To avoid flow separation at the leading edges of the flaps a Kutta condition is applied there which uniquely determines the angle of attack for a given flap configuration. The lift coefficient and lift-dependent drag factor are then calculated for this condition and compared with the prediction of slender thin-wing theory, in which the wing boundary condition is fully linearized.

Departmental Reference: Aero 3519

DTIC COPY INSPECTED 2

Accession For
NTIS GRA&I
DTIC TAB
Unannounced
Justification
By
Distribution/
Availability Codes
Dist | Avail and/or Special
A

Copyright
©
Controller HMSO London
1982

* School of Mathematics and Physics, University of East Anglia. This work was undertaken during a period at RAE under the CASE scheme.

LIST OF CONTENTS

1 INTRODUCTION

The idea of deflecting downwards the outboard part of a delta wing about a hinge-line or shoulder-line near the leading edge has been current for a considerable period[1,2]. It has been studied both as a simple form of built-in conical camber, intended to recover some part of the axial force which is lost through separation at the leading edge of a plane slender wing; and as a variable-geometry device, intended to enlarge the range of lift coefficient over which an acceptable performance can be achieved. Many measurements have confirmed that lower drag at lifting conditions can be obtained with such a leading-edge flap.

The benefit arises because the pressure differential across the wing is largest close to the leading edge, so that a downward deflection of the surface produces a force in the direction of flight. Since the downward deflection also reduces the size of the peak in the pressure differential, guidance is needed in the choice of an appropriate form and amount of deflection for a particular flight condition. Providing this guidance is not easy because, in general, the flow will separate at the leading edge of the wing to form a vortex.

However, if the angle of incidence is not too large, it is possible to droop each element of the leading edge in such a way that it points directly into the local on-coming flow, so that any tendency of the flow to separate at the leading edge is suppressed at this condition. In particular, if the flow past a delta wing is conical, this condition can be brought about by deflecting a leading-edge flap downwards about a straight hinge-line, the amount of deflection being greater for larger angles of incidence. For a wing at this 'attachment incidence' the flow can be calculated by the fully-linearized theory of attached flow, and it emerges that values of the lift-dependent drag not far above the minimum (corresponding to elliptic loading) are predicted for suitably designed wings. It also emerges in particular cases from both experiment[3] and calculation[4] that it is beneficial to use rather less leading-edge droop than would be required to achieve the condition of attached flow.

Despite the developments that have taken place in modelling the separated flow, based on slender-body theory and on panel methods, there is no adequate method for calculating the lift and drag of wings with small leading-edge vortices at subsonic speeds. It is therefore useful just to know how much droop of a particular form is needed to suppress the leading-edge separation. For the modest amount of built-in camber appropriate to a cruising condition, it appears[3,5] that a fully-linearized theory predicts this adequately. However, if a leading-edge flap, capable of deflection through large angles, is provided to improve performance at the much larger values of the lift coefficient associated with take-off and manoeuvre, it is not clear that the fully-linearized theory will be adequate, particularly as calculations[6] for a smoothly cambered wing revealed differences between the predictions of slender-body theory and the (fully-linearized) slender thin-wing theory. The present calculations were undertaken to discover how much deflection of a leading-edge flap is required to suppress leading-edge separation on a flat slender delta wing, and what lift coefficient and lift-dependent drag factor are predicted at this condition, and to assess how well these are predicted by the fully-linearized theory.

In the slender-body approximation the velocity potential satisfies Laplace's equation in two dimensions in each transverse or 'cross-flow' plane. The solution of this equation is achieved using complex variable techniques. We regard the cross-flow plane as being a complex plane and use a conformal transformation to map the region of the right-hand side of this plane outside the cross-section of the wing into the upper half of the transformed plane so that the half-wing is mapped onto the real axis of the transformed plane.

The geometrical parameters defining the wing, *ie* the flap length and deflection angle, lead to the aerodynamic properties of the configuration. The results are obtained by prescribing these two parameters and then calculating the required angle of attack to produce an attachment line on the leading edge: the lift and drag then follow.

2 STATEMENT OF THE PROBLEM

A cartesian coordinate system with origin at the apex of the wing is introduced. The x-axis lies along the wing centre line with the y-axis running to starboard and z-axis vertically upwards, so that the set $Oxyz$ is right-handed. The local semi-span is given by $s = Kx$, where $K = \tan\gamma$, and 2γ is the apex angle of the wing with flap undeflected. With a flap deflection β in the cross-flow plane $x = \text{constant}$, the configuration of Fig 1 is obtained. The apex angle of the undeflected part of the wing is $2\gamma'$, with the flap shoulder a distance $\bar{\eta}s$ from the wing centre line; $\bar{\eta}$ is thus a conical coordinate of the flap hinge-line. The flap length is therefore $(1-\bar{\eta})s$ and $\bar{\eta}K = \tan\gamma'$. The wing is shown in Fig 1 at incidence α to the undisturbed stream of velocity U, which is resolved into components $U\cos\alpha$ along Ox and $U\sin\alpha$ along Oz. These components are approximated by U and $U\alpha$ respectively. Hence, we seek a function ϕ such that the velocity potential Φ is given by

$$\Phi = Ux + \phi \quad . \tag{1}$$

Note that the extra term in the slender-body potential which takes into account the thickness of the configuration vanishes here as we are considering wings with no thickness.

Slender-body theory shows that the function ϕ satisfies the two-dimensional Laplace equation

$$\frac{\partial^2\phi}{\partial y^2} + \frac{\partial^2\phi}{\partial z^2} = 0$$

in each cross-flow plane. We are therefore treating the transverse velocity field as though the flow were two-dimensional, the three-dimensional nature of the problem only entering through the boundary conditions, which are that the velocity normal to the wing is zero, *ie*

$$\underline{n} \cdot \nabla\phi = 0 \tag{2}$$

where $\underline{n}$ is the unit outward normal to the wing, and that

$$\phi \sim Uz\alpha \tag{3}$$

at large distances from the wing.

We introduce new variables

$$\hat{y} = \frac{y}{s}, \quad \hat{z} = \frac{z}{s}, \quad \hat{\phi} = \frac{\phi}{Us} \tag{4}$$

and note that $\hat{\phi}$ satisfies Laplace's equation in the $(\hat{y},\hat{z})$ plane. We therefore seek a complex potential

$$W(Z) = \hat{\phi}(Z) + i\hat{\psi}(Z) \tag{5}$$

where $\hat{\psi}$ is the stream function corresponding to the potential $\hat{\phi}$, and $Z = \hat{y} + i\hat{z}$ is a non-dimensional complex coordinate in the cross-flow plane. The solution is obtained by conformally mapping the right-hand half of the Z-plane exterior to the cross-section of the wing onto the upper half of the t-plane so that the contour $A_\infty BCDEFA_\infty$ is mapped into the real axis of the t-plane (Fig 2). The potential $\hat{\phi}$ can then be found in the t-plane as that due to a distribution of sources on the real axis, together with a uniform flow, and inversion of the transformation will give the potential in the Z-plane.

3 THE TRANSFORMATION

We denote the image of L in the Z-plane by $\bar{L}$ in the t-plane. We may specify that $t = 0$ at $\bar{D}$ and denote the values of t at $\bar{B}$, $\bar{C}$, $\bar{E}$, $\bar{F}$ by b, c, e, f where

$$b < c < 0 < e < f \quad . \tag{6}$$

The required transformation is of the Schwartz-Christoffel type, whose general form is

$$\frac{dZ}{dt} = A\Pi(t - t_i)^{n_i} \quad ,$$

where t_i are the images of the vertices of the polygon in the Z-plane and the n_i are related to changes in direction of the contour at the vertices. Inserting the appropriate values of n_i and t_i gives

$$\frac{dZ}{dt} = A\frac{t}{\sqrt{(t-b)(t-f)}}\left(\frac{t-c}{t-e}\right)^{\beta/\pi} = AF(t) \tag{7}$$

where A is a constant. Then by substituting particular values of t and Z we obtain the following equalities:

$$\bar{\eta} = A\int_b^c F(t)dt \quad , \tag{8}$$

$$(1-\bar{\eta})e^{-i\beta} = A\int_c^0 F(t)dt \quad , \tag{9}$$

81150

$$(1-\bar{\eta})e^{-i(\beta+\pi)} = A\int_0^e F(t)dt \quad , \tag{10}$$

$$-\bar{\eta} = A\int_e^f F(t)dt \quad . \tag{11}$$

In evaluating the right-hand sides of equations (8) to (11) we must ensure the appropriate value is taken in the determination of the integrands as they are not single-valued functions. Writing $t = |t|e^{i\theta}$, $t-b = |t-b|e^{i\theta_b}$ etc, and $A = |A|e^{i\theta_a}$, we define

$$\frac{dZ}{dt} = \left|\frac{dZ}{dt}\right| e^{i\left(\theta+\theta_a-\frac{1}{2}\theta_b-\frac{1}{2}\theta_f+\frac{\beta}{\pi}\theta_c-\frac{\beta}{\pi}\theta_e\right)} \quad .$$

Then (8) gives:

$$\bar{\eta} = -\frac{A}{i}\int_b^c \frac{-t}{\sqrt{(t-b)(f-t)}}\left(\frac{c-t}{e-t}\right)^{\beta/\pi} dt \quad . \tag{12}$$

As the left-hand side of (12) is real and positive and the integral is real and positive we must choose A to be imaginary and negative to give the correct rotation between the Z- and t-planes. It is possible to choose $|A| = 1$, so preserving the boundary condition at infinity, because there is still some freedom in the transformation.

Hence

$$A = -i \tag{13}$$

and therefore

$$\int_b^c \frac{-t}{\sqrt{(t-b)(f-t)}}\left(\frac{c-t}{e-t}\right)^{\beta/\pi} dt = \bar{\eta} \tag{14}$$

where real, positive values of the radicals are intended. (9) to (11) give:

$$\int_c^0 \frac{-t}{\sqrt{(t-b)(f-t)}}\left(\frac{t-c}{e-t}\right)^{\beta/\pi} dt = 1-\bar{\eta} \quad , \tag{15}$$

$$\int_0^e \frac{t}{\sqrt{(t-b)(f-t)}}\left(\frac{t-c}{e-t}\right)^{\beta/\pi} dt = 1-\bar{\eta} \quad , \tag{16}$$

$$\int_e^f \frac{t}{\sqrt{(t-b)(f-t)}}\left(\frac{t-c}{t-e}\right)^{\beta/\pi} dt = \bar{\eta} \quad . \tag{17}$$

We now have in (14) to (17) four equations in four unknowns, b, c, e, f, depending on the two parameters $\bar{\eta}$ and β, giving a problem which is apparently determinate and capable of numerical solution.

However, before numerical treatment is possible the singularities in the integrands must be removed. To perform this we use the following substitutions:

in (14) put $t - b = r^2$,

in (16) put $e - t = r^k$, where $k = 1/(1 - (\beta/\pi))$,

and in (17) first put $f - t = r^2$,

and then put $f - e - r^2 = \bar{r}^k$, for $\frac{1}{2} \leqslant r \leqslant (f-e)^{\frac{1}{2}}$,

as the interval has to be split.

Equations (14) to (17) can be written in the form:

$$\underset{\sim}{F}(\underset{\sim}{x}) = 0 \ , \tag{18}$$

where $\underset{\sim}{F}$ is a vector of four nonlinear functions of the vector $\underset{\sim}{x} = (b,c,e,f)$. This system is solved by a multi-dimensional Newton scheme. The solution of (18) for the complete range of $\bar{\eta}$ and β is most easily obtained by keeping $\bar{\eta}$ constant and spanning the range of β. The solution for a pair $(\bar{\eta},\beta)$ can then be used as an initial guess at the solution for a neighbouring pair. The region of the $(\bar{\eta},\beta)$ parameter space which is physically and numerically accessible is discussed in section 5.

4 SOLUTION OF THE PROBLEM

4.1 Boundary conditions

The boundary condition on the undeflected part of the wing requires that $\hat{\phi}_{\hat{z}} = 0$ on that part of the contour. From the geometry in Fig 1 it can be shown that the unit outward normal to the flap is

$$\underset{\sim}{n} = \frac{1}{\sqrt{1 - \cos^2\beta \sin^2\gamma'}} \left(- \sin\beta \sin\gamma', \quad \sin\beta \cos\gamma', \quad \cos\beta \cos\gamma'\right) . \tag{19}$$

We require that the velocity normal to the flap is zero, so, by (1), (2) and (19), the velocity normal to the contour in the cross-flow plane is

$$\frac{\partial\phi}{\partial n} = \pm \frac{U \sin\beta \sin\gamma'}{\sqrt{1 - \cos^2\beta \sin^2\gamma'}} \ , \tag{20}$$

where the + and - refer to the upper and lower surfaces of the flap, respectively, and n is the distance normal to the contour.

Therefore the required non-dimensional normal velocity in the t-plane is

$$\left.\frac{\partial\hat{\phi}}{\partial\hat{n}}\right|_t = \left.\frac{\partial\hat{\phi}}{\partial\hat{n}}\right|_Z \left|\frac{dZ}{dt}\right| = \frac{1}{U}\frac{\partial\phi}{\partial n}\left|\frac{dZ}{dt}\right| = \pm\,\bar{\eta}K\sin\beta\left|\frac{dZ}{dt}\right| \tag{21}$$

where $\hat{n}$ is the non-dimensional distance normal to the contour, and higher-order terms in K have been neglected in the expansion of the right-hand side of (20), and here the $+$ and $-$ refer to the line segments $\overline{CD}$ and $\overline{DE}$, respectively. The normal velocity is zero elsewhere on the contour.

To realise this normal velocity we introduce a continuous non-dimensional source distribution in the t-plane with strength per unit length at t' given by

$$\left.\frac{d\hat{m}}{dt}\right|_{t'} = \left\{\begin{array}{ll} 2\bar{\eta}K\sin\beta\left|\frac{dZ}{dt}\right|_{t'}, & c < t' < 0, \\ -2\bar{\eta}K\sin\beta\left|\frac{dZ}{dt}\right|_{t'}, & 0 < t' < e, \\ 0, & \text{elsewhere.} \end{array}\right\} \tag{22}$$

We must also satisfy the boundary condition (3).

4.2 Complex potential

As stated in section 2 we shall form a complex potential, W, to satisfy the boundary conditions of section 4.1.

For the contribution from the source distribution (22) we obtain a complex potential W_1, where

$$\frac{dW_1}{dt} = 2\bar{\eta}K\sin\beta\int_{\mathscr{C}} \pm\frac{1}{2\pi}\left|\frac{dZ}{dt}\right|_{t'}\frac{1}{t-t'}\,dt', \tag{23}$$

where $\mathscr{C}$ is the curve $\overline{CE}$ in the t-plane, and the $+$ and $-$ refer to the portions of the curve stated previously.

To satisfy (3) we require

$$\frac{dW}{dZ} \sim -i\alpha \qquad \text{as} \quad |Z| \to \infty. \tag{24}$$

So (24) and (13) imply that

$$\frac{dW}{dt} \sim -\alpha \qquad \text{as} \quad |t| \to \infty$$

or

$$\frac{dW}{dt} = -\alpha + f(t) \tag{25}$$

where $|f(t)| \to 0$ as $|t| \to \infty$. The combined potential which satisfies (25) and gives the correct normal velocity as produced by (23) is

$$\frac{dW}{dt} = -\alpha + \frac{\bar{\eta}K \sin\beta}{\pi}\left(\int_c^0 - \int_0^e\right)\left|\frac{dZ}{dt}\right|_{t'} \frac{1}{t-t'}\,dt' \quad , \tag{26}$$

or

$$W = -\alpha t + \frac{\bar{\eta}K \sin\beta}{\pi}\left(\int_c^0 - \int_0^e\right)\left|\frac{dZ}{dt}\right|_{t'} \ln(t-t')dt' \quad . \tag{27}$$

4.3 Attachment condition

To avoid separation at the leading edge of the flap we impose a Kutta condition to remove the singularity in velocity and pressure. This will determine the value of α (α_a, say) that gives attached flow for a given flap configuration. For attachment we require that the velocity be finite at the leading edge, which, since $dZ/dt = 0$ there, leads to

$$\left.\frac{dW}{dt}\right|_{t=0} = 0 \quad . \tag{28}$$

Therefore from (26) and (7) we obtain (writing $t' = r$)

$$\alpha_a = \frac{\bar{\eta}K \sin\beta}{\pi}\left(\int_c^0 - \int_0^e\right)\left|\frac{Ar}{\sqrt{(r-b)(r-f)}}\left(\frac{r-c}{r-e}\right)^{\beta/\pi}\right|\frac{1}{-r}\,dr \quad , \tag{29}$$

and simplifying,

$$\frac{\alpha_a}{K} = \frac{\bar{\eta}\sin\beta}{\pi}\int_c^e \frac{1}{\sqrt{(r-b)(f-r)}}\left(\frac{r-c}{e-r}\right)^{\beta/\pi} dr \quad , \tag{30}$$

where again the singularity in the integrand must be removed by substituting $e - r = \bar{r}^k$ before numerical treatment can be applied.

We may also note at this point that a weaker singularity in the velocity and pressure exists at the shoulder of the flap and for moderate or large flap deflections we should expect separation at this point. However, this feature is being ignored in the present analysis and the potential flow calculated here predicts smooth flow around the shoulder with infinite velocity.

4.4 Lift

The lift can be obtained conveniently by the use of a distant control surface. If the non-dimensional complex potential W is expanded for large values of its non-dimensional argument Z in a plane of constant x, we obtain an expression of the form:

$$W = a_1 Z + a_0 + a_{-1}Z^{-1} + \ldots \quad . \tag{31}$$

The lift, L, acting on the portion of a thin wing upstream of the plane of constant x is then given in terms of the coefficient a_{-1} by a particular case of equation (9.7.11) of Ref 7 as

$$L = 2\pi\rho U^2 s^2 \mathcal{I}\{a_{-1}\} \quad . \tag{32}$$

Expansion of (7) for large t, followed by integration, shows that

$$Z = -i\left\{t + \gamma_0 + \bar{\gamma}\ \ell n\ t + \gamma_{-1} t^{-1} + O(t^{-2})\right\} \tag{33}$$

where $\bar{\gamma} = \frac{b}{2} - \frac{c\beta}{\pi} + \frac{e\beta}{\pi} + \frac{f}{2}$.

By a similar argument to Andrews[8] in his Appendix A it can be shown that the coefficient of $\ell n\ t$ in the expansion of Z (or that of $1/t$ in the expansion of dZ/dt) must vanish. Hence,

$$\frac{b}{2} - \frac{c\beta}{\pi} + \frac{e\beta}{\pi} + \frac{f}{2} = 0 \quad . \tag{34}$$

Using (34) we have

$$\gamma_{-1} = \frac{\beta^2}{2\pi^2}(e-c)^2 - \frac{\beta}{2\pi}(e-c)(e+c-b-f) - \frac{1}{8}(b-f)^2 \quad . \tag{35}$$

To invert (33) we write

$$t = i\left\{c_1 Z + c_0 + c_{-1} Z^{-1} + O(Z^{-2})\right\} \tag{36}$$

whence $$c_1 = 1\ , \quad c_0 = i\gamma_0\ , \quad c_{-1} = \gamma_{-1} \quad . \tag{37}$$

Expanding (27) for large t gives

$$W = -\alpha t + \frac{\bar{\eta} K \sin\beta}{\pi}\left(\int_c^0 - \int_0^e\right)\left|\frac{dZ}{dt}\right|_{t'}\left(\ell n\ t - \frac{t'}{t} + O(t^{-2})\right)dt' \quad , \tag{38}$$

but from (15) and (16)

$$\left(\int_c^0 - \int_0^e\right)\left|\frac{dZ}{dt}\right|_{t'} dt' = 0 \quad , \tag{39}$$

so introducing (36) and (37) into (38) and using (39) gives

$$W = -i\alpha\left(Z + i\gamma_0 + \gamma_{-1} Z^{-1}\right) + \frac{i\bar{\eta} K \sin\beta}{\pi Z}\left(\int_c^0 - \int_0^e\right)\left|\frac{dZ}{dt}\right|_{t'} t'dt' + O(Z^{-2}) \quad . \tag{40}$$

Hence

$$a_{-1} = -i\alpha\gamma_{-1} + \frac{i\bar{\eta}K \sin\beta}{\pi}\left(\int_c^0 - \int_0^e\right)\left|\frac{dZ}{dt}\right|_{t'} t'dt' \quad , \tag{41}$$

and so, at the attachment incidence, α_a ,

$$L_a = 2\pi s^2 \rho U^2 \left\{-\alpha_a\gamma_{-1} + \frac{\bar{\eta}K \sin\beta}{\pi}\left(\int_c^0 - \int_0^e\right)\left|\frac{dZ}{dt}\right|_{t'} t'dt'\right\} \quad . \tag{42}$$

A lift coefficient, C_{L_a} , based on the kinetic pressure, $\frac{1}{2}\rho U^2$, and the planform area of the wing with flap undeflected, s^2/K , is given by

$$\frac{C_{L_a}}{K^2} = 4\pi\left\{-\frac{\alpha_a\gamma_{-1}}{K} + \frac{\bar{\eta} \sin\beta}{\pi}\left(\int_c^0 - \int_0^e\right)\left|\frac{dZ}{dt}\right|_{t'} t'dt'\right\} \quad , \tag{43}$$

or simplifying the integral (writing $t' = r$)

$$\frac{C_{L_a}}{K^2} = 4\pi\left\{-\frac{\alpha_a\gamma_{-1}}{K} - \frac{\bar{\eta} \sin\beta}{\pi}\int_c^e \frac{r^2}{\sqrt{(r-b)(f-r)}}\left(\frac{r-c}{e-r}\right)^{\beta/\pi} dr\right\} \quad , \tag{44}$$

where γ_{-1} is given by (35). Here also the singularity in the integrand must be removed for numerical purposes, as before.

In the Appendix, equation (44) is expanded for small values of β , and it is verified that the leading term agrees with the expression obtained from the fully-linearized slender thin-wing theory, in which the wing and flap boundary condition is applied in the plane $z = 0$.

4.5 Drag

The drag is obtained by first calculating the normal force on the flap. The overall drag can then be calculated by resolving the normal forces on the wing and flap as shown later. The normal force on the flap is evaluated by integrating the pressure jump across it: the pressure is obtained from the velocity components on the flap. The entire force comes from the pressure integral as there is no localised suction force on the leading edge as we are considering the attachment incidence only.

If $\hat{u}$ and $\hat{v}$ are the non-dimensional velocity components in the t-plane, then from (26), (21) and (27):

$$\hat{u} = -\alpha + \frac{\bar{\eta}K \sin\beta}{\pi}\left(\int_c^0 - \int_0^e\right)\left|\frac{dZ}{dt}\right|_{t'} \frac{1}{t-t'}\,dt' \tag{45}$$

$$\hat{v} = \begin{cases} \bar{\eta}K \sin\beta \left|\dfrac{dZ}{dt}\right| , & c < t < 0 ; \\ -\bar{\eta}K \sin\beta \left|\dfrac{dZ}{dt}\right| , & 0 < t < e ; \end{cases} \tag{46}$$

and

$$\hat{\phi} = -\alpha t + \frac{\bar{\eta}K \sin\beta}{\pi}\left(\int_c^0 - \int_0^e\right)\left|\frac{dZ}{dt}\right|_{t'} \ell n|t-t'|dt' \quad . \tag{47}$$

The evaluation of (45) involves calculating a Cauchy Principal Value integral which is performed by subtracting out the singularity to give

$$\hat{u} = -\alpha + \frac{\bar{\eta}K \sin\beta}{\pi}\left(\int_c^0 - \int_0^e\right)\left\{\left|\frac{dZ}{dt}\right|_{t'} - \left|\frac{dZ}{dt}\right|_t\right\}\frac{1}{t-t'}\,dt' + \frac{\bar{\eta}K \sin\beta}{\pi}\left|\frac{dZ}{dt}\right| \ell n\left|\frac{(t-c)(t-e)}{t^2}\right| . \tag{48}$$

Although the integrand in (47) is integrable, for numerical purposes a first-order estimate of the integral in the region of the logarithmic singularity is made separately.

Then

$$\frac{\phi_y - i\phi_z}{U} = \hat{\phi}_{\hat{y}} - i\hat{\phi}_{\hat{z}} = \frac{dW}{dZ} = (\hat{u} - i\hat{v})\frac{dt}{dZ} , \tag{49}$$

and as the flow is conical

$$\phi_x = \frac{1}{x}\left(\phi - y\phi_y - z\phi_z\right) = KU\left(\hat{\phi} - \hat{y}\hat{\phi}_{\hat{y}} - \hat{z}\hat{\phi}_{\hat{z}}\right) , \tag{50}$$

from Euler's theorem on homogeneous functions.

The pressure coefficient, according to slender-body theory, is given by

$$C_p = \frac{p - p_\infty}{\frac{1}{2}\rho U^2} = 1 - \frac{\nabla\phi\nabla\phi}{U^2} = \alpha^2 - \frac{2\phi_x}{U} - \frac{\left(\phi_y^2 + \phi_z^2\right)}{U^2}$$

or

$$\frac{C_p}{K^2} = \left(\frac{\alpha}{K}\right)^2 - \frac{2\phi_x}{K^2U} - \frac{\left(\phi_y^2 + \phi_z^2\right)}{K^2U^2} , \tag{51}$$

and can be evaluated from the velocity components given in (49) and (50).

The coefficient of normal force on one flap, C_{NF}, then follows by integrating the jump in pressure coefficient, ΔC_p, over the flap, and non-dimensionalising with the wing area with flaps undeflected to give

$$C_{NF} = \frac{1}{sx} \int_0^x \left\{ \int_{\bar{\eta}s}^{s} \Delta C_p \, d\xi \right\} dx \quad ,$$

where ξ is measured along the flap. Using the fact that pressure is constant along conical rays and writing $\xi = \zeta s$ gives

$$\frac{C_{NF}}{K^2} = \frac{1}{2} \int_{\bar{\eta}}^{1} \frac{\Delta C_p}{K^2} \, d\zeta \quad . \tag{52}$$

From (19) the components of C_{NF} in the x and z directions are, taking leading order terms, $-\sin\beta\,\bar{\eta}KC_{NF}$ and $\cos\beta\,C_{NF}$ respectively. The coefficient of normal force on the undeflected part of the wing is then $C_{L_a} - 2\cos\beta\,C_{NF}$. To obtain the drag it is necessary to resolve these components of force in the free-stream direction so that the drag coefficient (based on the area of the wing with undeflected flaps) at the attachment incidence is given by (for the slender-body approximation of small α)

$$C_{D_a} = \left(C_{L_a} - 2\cos\beta\,C_{NF}\right)\alpha_a + 2\cos\beta\,C_{NF}\alpha_a - 2\bar{\eta}K\sin\beta\,C_{NF} \quad ,$$

or

$$\frac{C_{D_a}}{K^3} = \frac{C_{L_a}}{K^2}\frac{\alpha_a}{K} - 2\bar{\eta}\sin\beta\,\frac{C_{NF}}{K^2} \quad . \tag{53}$$

A measure of the lifting performance of the wing is then given by the lift-dependent drag factor, χ, where

$$\chi = \frac{\pi A C_D}{C_L^2} = \frac{4\pi K C_D}{C_L^2} = \frac{4\pi C_D}{K^3}\left(\frac{C_L}{K^2}\right)^{-2} \quad , \tag{54}$$

and where here, A is the aspect ratio of the wing with undeflected flaps.

It is of course possible to obtain the force on the undeflected part of the wing by integrating the pressure jump over this region in a similar way to that described above: the main differences are that, in (45) the integral is no longer of the Cauchy Principal Value type; (46) becomes $v = 0$; and in (47) no logarithmic singularity is involved in the integrand. This was done for a few cases, firstly to obtain a complete picture of the pressure distribution on the wing and secondly to provide a check on the method, since the total force in the z-direction should equal the lift as calculated in section 4.4.

5 RESULTS

The geometry of the wing imposes bounds on the physically attainable parameter space $(\bar{\eta},\beta)$. For $\bar{\eta} < 0.5$ the opposite flaps will meet before $\beta = \pi$. In fact the maximum angle of deflection possible for a given $\bar{\eta}$ is

$$\beta_{max} = \cos^{-1}\left(\frac{\bar{\eta}}{\bar{\eta} - 1}\right) \qquad 0 \leq \bar{\eta} \leq 0.5,$$

$$= \pi \qquad 0.5 \leq \bar{\eta} \leq 1.0.$$

The boundary of the parameter space is shown in Fig 3 together with the region covered numerically. Difficulties arose in the convergence of the Newton scheme for finding the parameters b, c, e, f in the transformation near the $(\bar{\eta},\beta)$ boundary for $\bar{\eta} < 0.5$. This was due to $\bar{E}$ and $\bar{F}$ coalescing on the boundary, so that, in the course of the iteration, e became greater than f, violating (6).

The values of the incidence parameter at the attachment condition, α_a/K, are shown in Fig 4 over the range of values of β and $\bar{\eta}$ for which solutions have been obtained. As would be expected, the attachment incidence increases as the deflection increases, up to quite large deflection angles. However, if $\bar{\eta} > 0.5$, so that the flaps can be deflected right back under the wing, the attachment incidence eventually falls again as the deflection angle approaches π. In the limit, the wing is again a flat plate, giving a mathematical check, despite the physical unreality of the flow model. The condition that the flow attaches at the leading edge of the flap now expresses that the flap leading edge is an attachment line on the lower surface of the wing. The non-dimensional coordinate, η_A, of the attachment line (*ie* the distance of the attachment line from the centre line divided by the local semi-span), on the lower surface of a slender flat-plate delta wing is given by

$$\eta_A = \left[1 - \left(\frac{\alpha}{K}\right)^2\right]^{\frac{1}{2}}, \qquad \text{for } \frac{\alpha}{K} \leq 1,$$

$$\eta_A = 0, \qquad \text{for } \frac{\alpha}{K} > 1;$$

see *eg* Ref 9.

The semi-span of the new wing, consisting of the undeflected portion of the original wing, is, of course, $\bar{\eta}s$. The flap leading edge is $s(1 - \bar{\eta})$ inboard of the new leading edge (the old hinge line) and so

$$\eta_A = \frac{\bar{\eta}s - s(1 - \bar{\eta})}{\bar{\eta}s} = \frac{2\bar{\eta} - 1}{\bar{\eta}}.$$

Moreover K in the equations above must be replaced by $\tan\gamma' = K\bar{\eta}$. Then

$$\frac{\alpha_a}{K} = \bar{\eta}\sqrt{1 - \eta_A^2} = \sqrt{(1 - \bar{\eta})(3\bar{\eta} - 1)} \qquad \text{for } \bar{\eta} > 0.5 \qquad (55)$$

or

$\bar{\eta}$	0.6	0.7	0.8	0.9
α_a/K	0.5657	0.5745	0.5292	0.4123

These values of α_a/K at $\beta = \pi$, taken with the computed results in Fig 4, imply a very rapid variation as β tends to π, which is a plausible behaviour.

The practically relevant values of β are less than $\pi/2$, for which the presentation in Fig 4 is confused. Fig 5 shows the variation of $\alpha_a/\beta K$ with β for fixed values of $\bar{\eta}$. The values at $\beta = 0$ correspond to the fully-linearized theory (Appendix). From equation (A-1) we find that, for the linear theory, $\alpha_a/\beta K$ is a maximum for $\bar{\eta} = 0.652$, taking the value 0.3572. Fig 5 shows that for $\beta > 0$, a larger maximum is obtained at a smaller value of $\bar{\eta}$. For $\bar{\eta} \leq 0.8$, the attachment incidence grows more rapidly with β than the linear theory predicts; for $\bar{\eta} = 0.9$ it grows less rapidly. If $\bar{\eta} = 0$, so that only the flaps remain, we have a 'caret wing' configuration. As $\bar{\eta} \to 0$, $e \to f$ and in (30) two singularities of the integrand coalesce, the integral remaining finite for $\beta < (\pi/2)$; the attachment incidence thus tends to zero.

The comparison with linear theory is brought out more clearly in Fig 6, where the ratio of the 'exact' attachment incidence to its linear estimate is plotted against β for fixed values of $\bar{\eta}$. For inboard positions of the hinge line, large errors appear, but for the most practical positions at 80% and 90% of the semi-span, the linear theory prediction is within 5% for deflection angles up to 90°. Even for a hinge line at 60% semi-span, which is probably the furthest inboard that could be contemplated on a real configuration, the error is within 10% up to a deflection of 50° and only exceeds 30% at deflections above 85°. At first sight, the accuracy achieved by the linear theory is surprising. However, it must be remembered that the linear result is obtained by applying the boundary conditions on that part of the plane occupied by the wing with the flap undeflected. This is not the procedure adopted in the application of linear theory to cambered and twisted wings, in which the boundary condition is applied on the projection of the wing onto its mean plane. If the conventional procedure were applied, it would clearly produce a substantial underestimate of the attachment incidence for the larger deflection angles.

The lift coefficient at the attachment condition, in its similarity form C_{L_a}/K^2, is shown in Fig 7, again as a function of β for fixed values of $\bar{\eta}$. For the larger values of β there is a general resemblance to the curves in Fig 4. In particular the same rapid variation near $\beta = \pi$ arises. The values for $\beta = \pi$ follow from the familiar expression for the lift of a flat slender wing,

$$L = \pi\rho U^2 s^2 \alpha \quad .$$

By replacing s by $\bar{\eta}s$ and introducing $S = s^2/K$ and α_a from (55)

$$\frac{C_{L_a}}{K^2} = 2\pi\bar{\eta}^2 \frac{\alpha_a}{K} = 2\pi\bar{\eta}^2\sqrt{(1-\bar{\eta})(3\bar{\eta}-1)} \ ,$$

or

$\bar{\eta}$	0.6	0.7	0.8	0.9
C_{L_a}/K^2	1.280	1.769	2.128	2.098

For the smaller values of β, the lift varies more rapidly with $\bar{\eta}$ than does the attachment incidence.

The variation for the smaller values of β is brought out more clearly in Fig 8, where $C_{L_a}/\beta K^2$ is shown for $0 \leq \beta \leq 1.5$. The values at $\beta = 0$ correspond to the fully-linearized theory given by equation (A-3). It is easy to see from this equation that, for a given deflection angle, the linear theory predicts a maximum value of C_L at $\bar{\eta} = \left(\frac{2}{3}\right)^{\frac{1}{2}} = 0.816$. The present calculations show that a hinge position near 80% of the semi-span is close to the optimum for deflection angles up to 90°, though little is lost by any choice between 70% and 90%.

It is apparent from Fig 8 that the linearized approximation, in which the curves are replaced by horizontal lines, is a very good one, particularly for the three most outboard positions of the hinge line, which are also those of most practical interest. The points indicated on the curves show the extent of the range for which the linearized result is within 5% of the exact value.

The lift-dependent drag factor, χ, is shown in Fig 9 for the three most outboard hinge positions, *ie* $\bar{\eta} = 0.7$, 0.8 and 0.9, and for flap deflections up to 120°. It may be noted here that calculation of the drag caused certain problems, not least being that a very fine subdivision of the flap was necessary in the numerical evaluation of the integral of the pressure jump across the flap (equation (52)) to achieve a relatively low accuracy in the normal force: the problem worsened as deflection and flap length increased. This difficulty ultimately limited the parameter space that was covered, for the lift-dependent drag factor, because the computational times increased beyond acceptable limits. However, the most physically realistic cases fall within the region of the $(\bar{\eta},\beta)$ space covered by the calculations.

Again comparison is drawn between the linearized boundary condition results (dashed line) given by equation (A-8) and the 'exact' boundary conditions (continuous line), with the points indicated having the same meaning as stated above for the lift. Here, also, the linearized approximation is seen to be very good for these cases, with any flap deflection up to 45° being within the 5% error band for all three hinge positions. Moving the hinge line outboard increases the range for which the error in the approximation is small.

It must be emphasized that all coefficients have been referred to the area of the basic wing with undeflected flap, and it is the aspect ratio of this wing which appears in

the definition of χ . Consequently, the solid lines in Fig 9 show the reduction in lifting efficiency which results from increasing the flap deflection on a given wing so as to maintain the attachment condition at increasing values of the incidence or lift coefficient: the broken lines are calculated on the same basis. A very different picture arises if the flap deflection is regarded as a form of conical camber applied to a wing of a given planform, *ie* given projected area in the plane $z = 0$. If χ is written in terms of the drag, D , the lift, L , and the semi-span, s , the result is

$$\chi = \frac{2\pi\rho U^2 s^2 D}{L^2} \quad .$$

Consequently, if the wing remains the same, with the same forces acting on it, but the span is defined differently, χ changes. In particular, if the span of the planform is used in place of the span of the basic wing with the undeflected flap, χ is reduced by a factor $(\bar{\eta} + (1 - \bar{\eta}) \cos \beta)^2$. For the rather extreme example of $\bar{\eta} = 0.7$, $\beta = (\pi/2)$, this means reducing the value of 1.71 shown in Fig 9 to 0.84. This value is comparable with those found for large amounts of conical camber of circular arc form in Ref 6.

Figs 10, 11 and 12 show the pressure distribution over the whole wing (drawn with the flap undeflected for ease of presentation) for the cases $\bar{\eta} = 0.7$, $\beta = 0.5$ and $\bar{\eta} = 0.8$, $\beta = 0.5$ and $\beta = 1.1$. As stated earlier, the suction at the hinge-line on the upper surface is infinite although no localised suction force is present for flap deflections below $\beta = \pi$. For the cases with the same flap deflection the lifts are similar and the loading can be seen to be of a similar magnitude. For the larger flap deflection the loading both on the undeflected part of the wing and on the flap itself is appreciably larger than for the smaller deflection for the same hinge-line position.

All the results obtained are affected by the limited applicability of slender-body theory. For Mach numbers greater than unity, the linearized theory of supersonic flow provides useful guidance. Equation (A-2) shows that the lift of a delta wing with a slightly deflected leading-edge flap at its attachment condition increases as the Mach number increases above unity. The close agreement between the present calculations and the fully-linearized expression (A-3) suggests that (A-2) is likely also to be a useful approximation for large flap deflections, provided the leading edges are not too close to the Mach cone from the apex. For subsonic speeds no such simple result is possible; since the flow over the conical configuration will no longer be conical, there will be no incidence at which the flow will be attached along the whole leading edge. Practically this seems to be unimportant. For instance, a wing of aspect ratio 0.75, with a gothic planform, 8.25% thick on the centre line, with camber and twist designed by slender theory for attached flow at a lift coefficient of 0.1, was found[10] to show no signs of leading-edge separation at low speeds at lift coefficients of 0.09 and 0.15.

6 CONCLUSIONS

The application of slender-body theory to a delta wing furnished with a conical leading-edge flap, deflected so as to maintain attached flow at the leading edge, shows the following:

(1) Increasing the angle of deflection, measured in the cross-flow plane, up to 90° and beyond produces an increasing angle of incidence for attachment and an increasing lift coefficient at the attachment condition. At the same time, there is a decrease in the lifting efficiency, as measured by a lift-dependent drag factor based on the planform of the wing with the flap undeflected.

(2) The fully-linearized slender thin-wing theory agrees fairly well with the slender-body theory for the practical cases of outboard hinge-lines. The lift at attachment is predicted particularly closely by the linear theory for hinge lines at 70%, 80% and 90% of the semi-span, where the error is less than 5% for deflection angles up to 75°. The lift-dependent drag factor is within the same tolerance for deflection angles up to 45°, for the same hinge-line positions.

(3) The largest lift coefficients at attachment for a given deflection angle are produced with the hinge-line near 80% of the semi-span, but the degradation at 70% and 90% is small. For this hinge-line position, the lift coefficient at attachment is about $1.5\ \beta K^2$, where K is the tangent of the semi-apex angle and β is the deflection angle (in radians), for $\beta \leq (\pi/2)$.

Appendix

LINEARIZED BOUNDARY CONDITIONS

Smith and Mangler[11] calculated the supersonic flow over a delta wing with hinged flaps at the subsonic leading edges using linearized boundary conditions. Their result (in closed form) for the attachment incidence is

$$\alpha_a = -\frac{\xi}{\pi}\, 2a^2 \Pi \frac{\bar{\eta}\sqrt{1-\bar{\eta}^2}}{\sqrt{1-a^2\bar{\eta}^2}}$$

where here $a = \tan\gamma/\tan\mu$, where $\mu = \operatorname{cosec}^{-1} M$ is the Mach angle, M being the Mach number, and

$$\Pi = \Pi\left(a^2\bar{\eta}^2 - 1\,,\quad \sqrt{1-a^2}\right)$$

is the complete elliptical integral of the third kind. In this case $\xi = -\bar{\eta}K\beta$. The slender wing corresponds to the limit $a = 0$. Taking this limit we find that

$$\frac{\alpha_a}{K\beta} = \frac{2\bar{\eta}\cos^{-1}\bar{\eta}}{\pi} \quad . \tag{A-1}$$

The lift coefficient is stated to be

$$C_{L_a} = -\frac{4\xi\bar{\eta}\tan\gamma\sqrt{1-\bar{\eta}^2}}{\sqrt{1-a^2\bar{\eta}^2}} \tag{A-2}$$

which yields, on taking the same limit

$$\frac{C_{L_a}}{K^2\beta} = 4\bar{\eta}^2\sqrt{1-\bar{\eta}^2} \quad . \tag{A-3}$$

We now show that these expressions, (A-1) and (A-3), are obtained from the present treatment by retaining terms of leading order in β only. Equation (30) shows that α_a/K is proportional to β when β is small, so the integral in (30) may be evaluated for $\beta = 0$ if only the leading term is needed. By the same argument, in (44) it is adequate to evaluate the integral and the coefficient γ_{-1} for $\beta = 0$. Then by (35)

$$\bar{\gamma}_{-1} = -\tfrac{1}{8}(\bar{b} - \bar{f})^2 \tag{A-4}$$

where the overbar denotes the quantity evaluated for $\beta = 0$. To find $\bar{b}$, $\bar{c}$, $\bar{e}$, $\bar{f}$ we put $\beta = 0$ in (14) to (17). Adding (16) and (17) and subtracting (14) and (15) gives

81150 0150

$$\int_{\bar{b}}^{\bar{f}} \frac{t}{\sqrt{(t-\bar{b})(\bar{f}-t)}}\,dt = 0 \ .$$

With $t = \bar{b}\cos^2\theta + \bar{f}\sin^2\theta$, the integral reduces to

$$2\int_0^{\pi/2} (\bar{b}\cos^2\theta + \bar{f}\sin^2\theta)d\theta = \frac{\pi}{2}(\bar{b}+\bar{f})$$

and so $\bar{b} = -\bar{f}$. Now adding (16) and (17), again with $\beta = 0$, gives

$$\int_0^{\bar{f}} \frac{t}{\sqrt{\bar{f}^2 - t^2}}\,dt = 1 \ .$$

With $t = \bar{f}\sin\theta$, the integral reduces to $\bar{f}$, so $\bar{f} = 1$. Equation (17) reduces to

$$\int_{\bar{e}}^{1} \frac{t}{\sqrt{1-t^2}}\,dt = \bar{\eta}$$

from which $\bar{e} = \sqrt{1-\bar{\eta}^2}$. By inspection of (15) and (16)

$$\bar{c} = -\bar{e} \ .$$

The integral in (30) becomes

$$\int_{\bar{c}}^{\bar{e}} \frac{dt}{\sqrt{1-t^2}} = \sin^{-1}\bar{e} - \sin^{-1}\bar{c} = 2\cos^{-1}\bar{\eta}$$

and so

$$\frac{\alpha_a}{K} = \frac{2\beta\bar{\eta}\cos^{-1}\bar{\eta}}{\pi} \qquad \text{(A-5)}$$

to leading order. The integral in (44) becomes

$$\int_{\bar{c}}^{\bar{e}} \frac{t^2}{\sqrt{1-t^2}}\,dt = \cos^{-1}\bar{\eta} - \bar{\eta}\sqrt{1-\bar{\eta}^2}$$

and so, using (A-3) we have

$$\frac{C_{L_a}}{K^2} = 4\pi \left\{ \frac{2\beta\bar{\eta}\cos^{-1}\bar{\eta}}{\pi}\frac{1}{2} - \frac{\beta\bar{\eta}}{\pi}\left(\cos^{-1}\bar{\eta} - \bar{\eta}\sqrt{1-\bar{\eta}^2}\right)\right\} = 4\beta\bar{\eta}^2\sqrt{1-\bar{\eta}^2} \quad . \tag{A-6}$$

Equations (A-5) and (A-6) agree with (A-1) and (A-3), providing a partial check on the present formulation.

The expression for the drag using the linearized boundary condition is, on taking the slender-body limit,

$$\frac{C_{D_a}}{K^3} = -\frac{8}{\pi}\bar{\eta}^4\beta^2 \log\bar{\eta} \tag{A-7}$$

which on combining with (A-6) gives a lift-dependent drag factor

$$\chi = \frac{4\pi K C_D}{C_L^2} = -\frac{2\log\bar{\eta}}{(1-\bar{\eta}^2)} \quad . \tag{A-8}$$

81150
81150

LIST OF SYMBOLS

A	constant in transformation, also aspect ratio of wing with undeflected flap
a	$= \tan\gamma/\tan\mu$ (see Appendix)
a_i	constants in expansion of W in terms of Z
b,c,e,f	coordinates of $\bar{B}$, $\bar{C}$, $\bar{E}$, $\bar{F}$
C_L	lift coefficient based on total area of wing and flaps
C_{L_a}	lift coefficient at incidence for attachment, α_a
C_{NF}	normal force coefficient on flap
C_p	pressure coefficient
C_{D_a}	drag coefficient at incidence for attachment
c_i	constants in expansion of t in terms of Z
D	drag
i	$= \sqrt{-1}$
K	$= \tan\gamma$
k	$= 1/(1-(\beta/\pi))$
L	lift
L_a	lift at attachment incidence, α_a
M	Mach number (see Appendix)
$\hat{m}$	source strength
$n,\hat{n}$	distance and non-dimensional distance normal to contour
$\underline{n}$	unit outward normal to wing
S	wing area with flaps undeflected
s	semi-span of cross-section with flaps undeflected
t	complex coordinate in transformed plane
U	free stream velocity
$\hat{u}-i\hat{v}$	complex velocity in t-plane (non-dimensional)
W,W_1	complex potentials
x,y,z	cartesian coordinates
$\hat{y},\hat{z}$	$= y/s$, z/s, non-dimensional coordinates
Z	$= (y+iz)/s$, non-dimensional complex coordinate in cross-flow plane

LIST OF SYMBOLS (concluded)

α	incidence
α_a	incidence for attachment
β	flap deflection in cross-flow plane
γ	semi-apex angle of wing with flap undeflected
γ'	semi-apex angle between hinge lines
$\gamma_i, \bar{\gamma}$	constants in expansion of Z in terms of t
η_A	non-dimensional coordinate of attachment line, equation (55)
$\bar{\eta}$	conical coordinate of the flap hinge-line
μ	= $\text{cosec}^{-1} M$, the Mach angle (see Appendix)
ρ	density
Φ	velocity potential
ϕ	cross-flow potential
$\hat{\phi}$	= ϕ/Us , non-dimensional potential
$\hat{\psi}$	stream function corresponding to $\hat{\phi}$
χ	lift-dependent drag factor, equation (54)

81150
05118

REFERENCES

No.	Author	Title, etc
1	B.W.B. Shaw	Nose controls on delta wings at supersonic speeds. College of Aeronautics, Cranfield, Rep No.36, ARC 13372 (1950)
2	J.F. Marchman E.B. Plentovich D. Manor	Performance improvement on delta wings at supersonic speeds due to vortex flaps. J. Aircraft 18, 4, 280-6 (1981)
3	P.J. Butterworth	Low speed wind-tunnel tests on a family of cambered wings of mild gothic planform of aspect ratio 1.4. RAE Technical Report 70185 (1970) ARC CP 1163 (1970)
4	J.E. Barsby	Flow past conically cambered slender delta wings with leading edge separation. RAE Technical Report 72179 (1972) ARC R&M 3748 (1972)
5	L.C. Squire	A review of experimental work on the aerodynamics of integrated slender wings for supersonic flight. RAE Technical Report 80069 (1980)
6	J.H.B. Smith	The properties of a thin conically cambered wing according to slender-body theory. RAE Report Aero 2602 (1958) ARC R&M 3135 (1960)
7	G.N. Ward	Linearized theory of steady high-speed flow. CUP (1955)
8	R.D. Andrews	Calculation of the lift of slender rectangular-fuselage-high-wing combinations. RAE Technical Report 68300 (1968) Aero J. 74, No.719, 903-6 (1970)
9	J.H.B. Smith	Remarks on the structure of conical flow. Progress in Aerospace Sciences, Vol.12, Oxford, Pergamon Press (1972)
10	R.F.A. Keating	Low speed wind-tunnel tests on sharp-edged gothic wings of aspect ratio 3/4. RAE Technical Note Aero 2686 (1961) ARC CP 576 (1961)
11	J.H.B. Smith K.W. Mangler	The use of conical camber to produce flow attachment at the leading edge of a delta wing to minimize lift-dependent drag at subsonic and supersonic speeds. RAE Report Aero 2584 (1957) ARC R&M 3289 (1957)

REPORTS QUOTED ARE NOT NECESSARILY AVAILABLE TO MEMBERS OF THE PUBLIC OR TO COMMERCIAL ORGANISATIONS

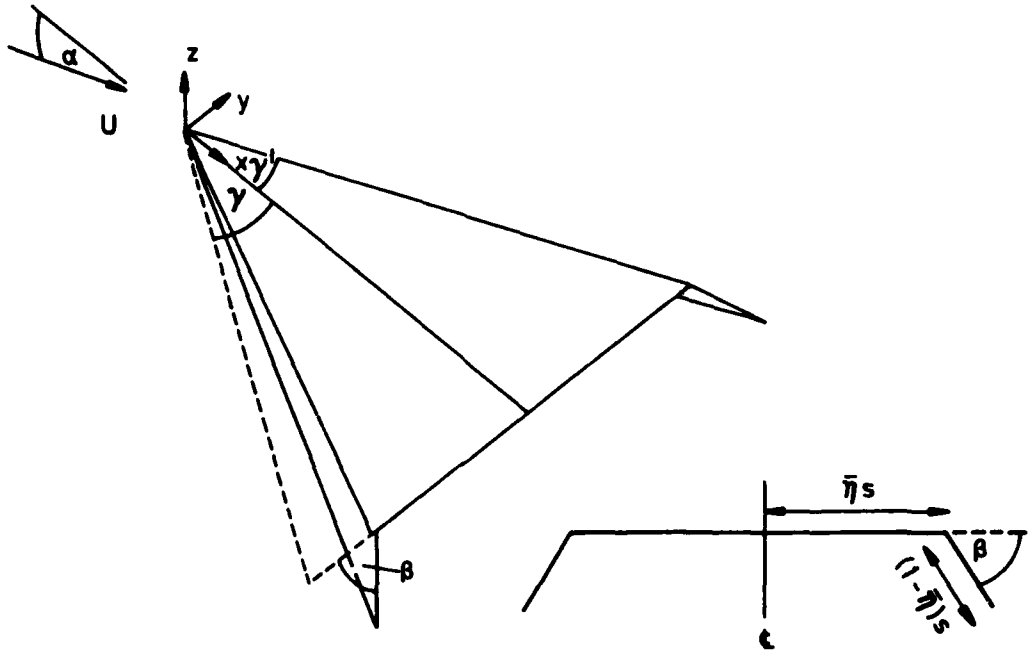

Fig 1 Flapped wing – overall view and cross-section

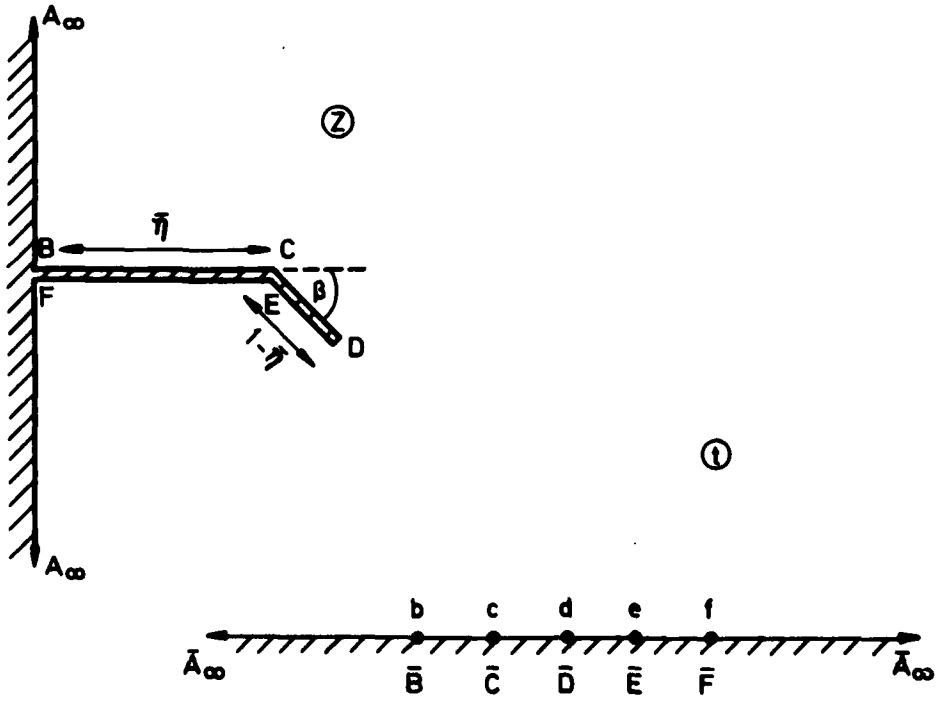

Fig 2 The non-dimensional complex cross-flow (Z) plane and the transformed (t) plane

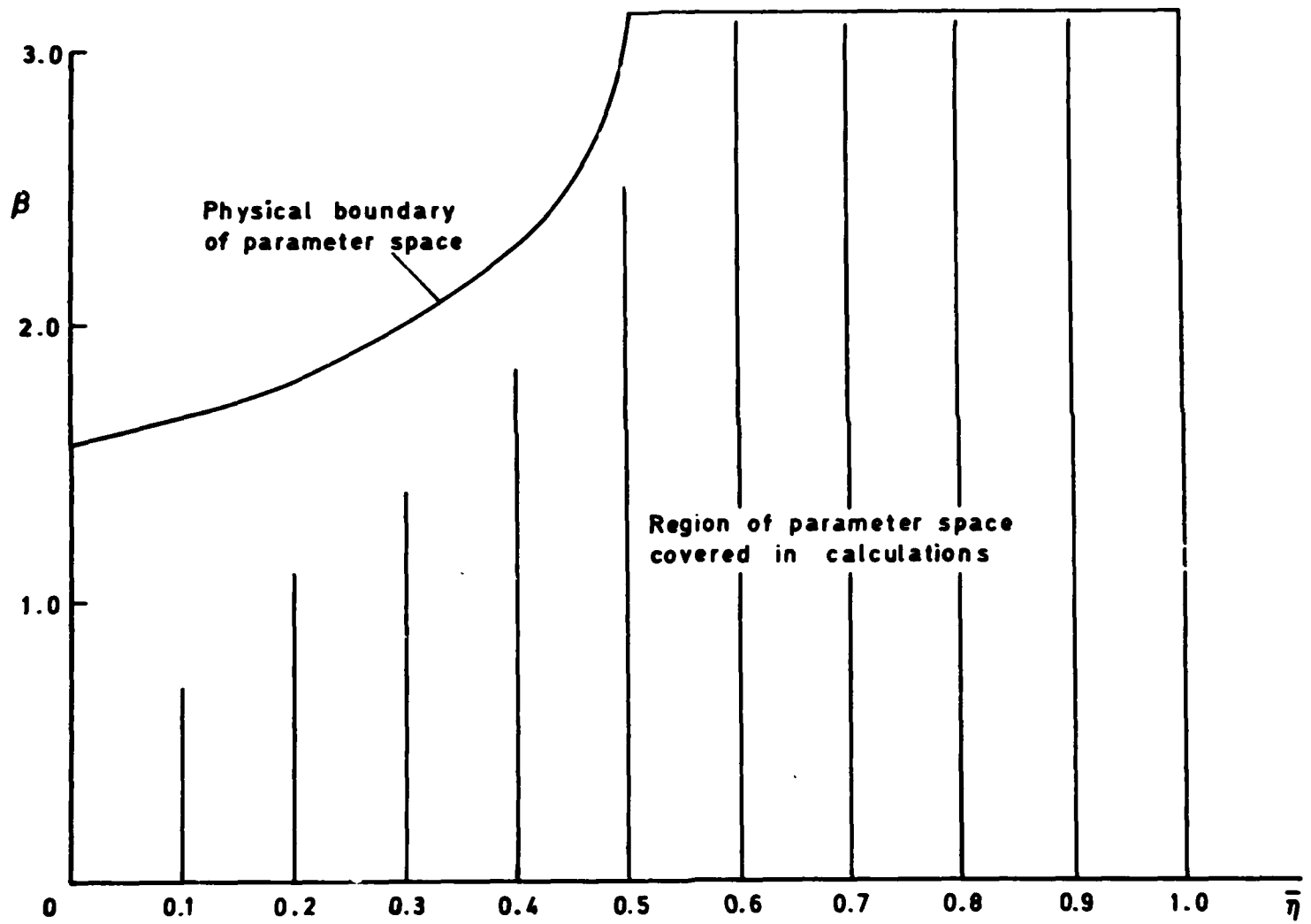

Fig 3 Regions of the parameter space

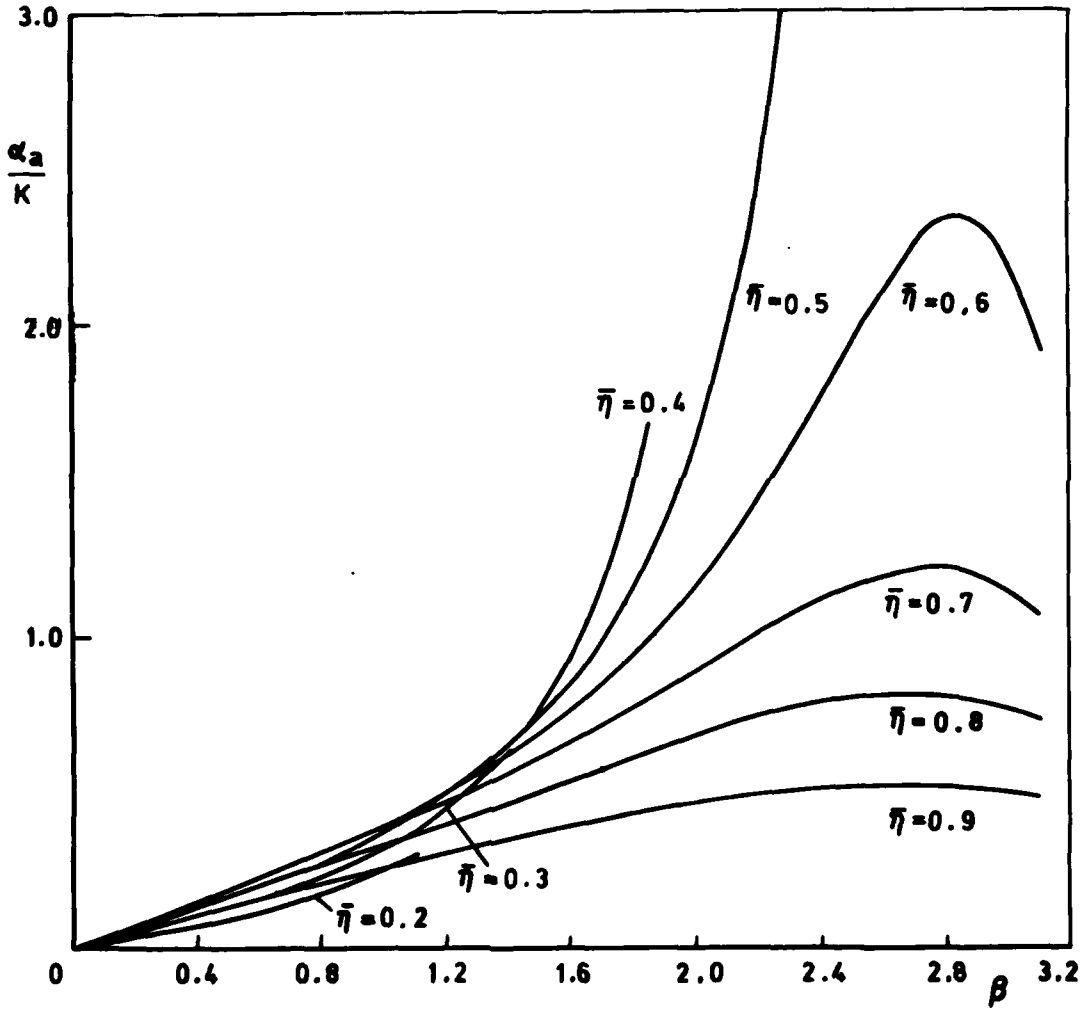

Fig 4 Variation of α_a/K with β for various $\bar{\eta}$

Fig 5

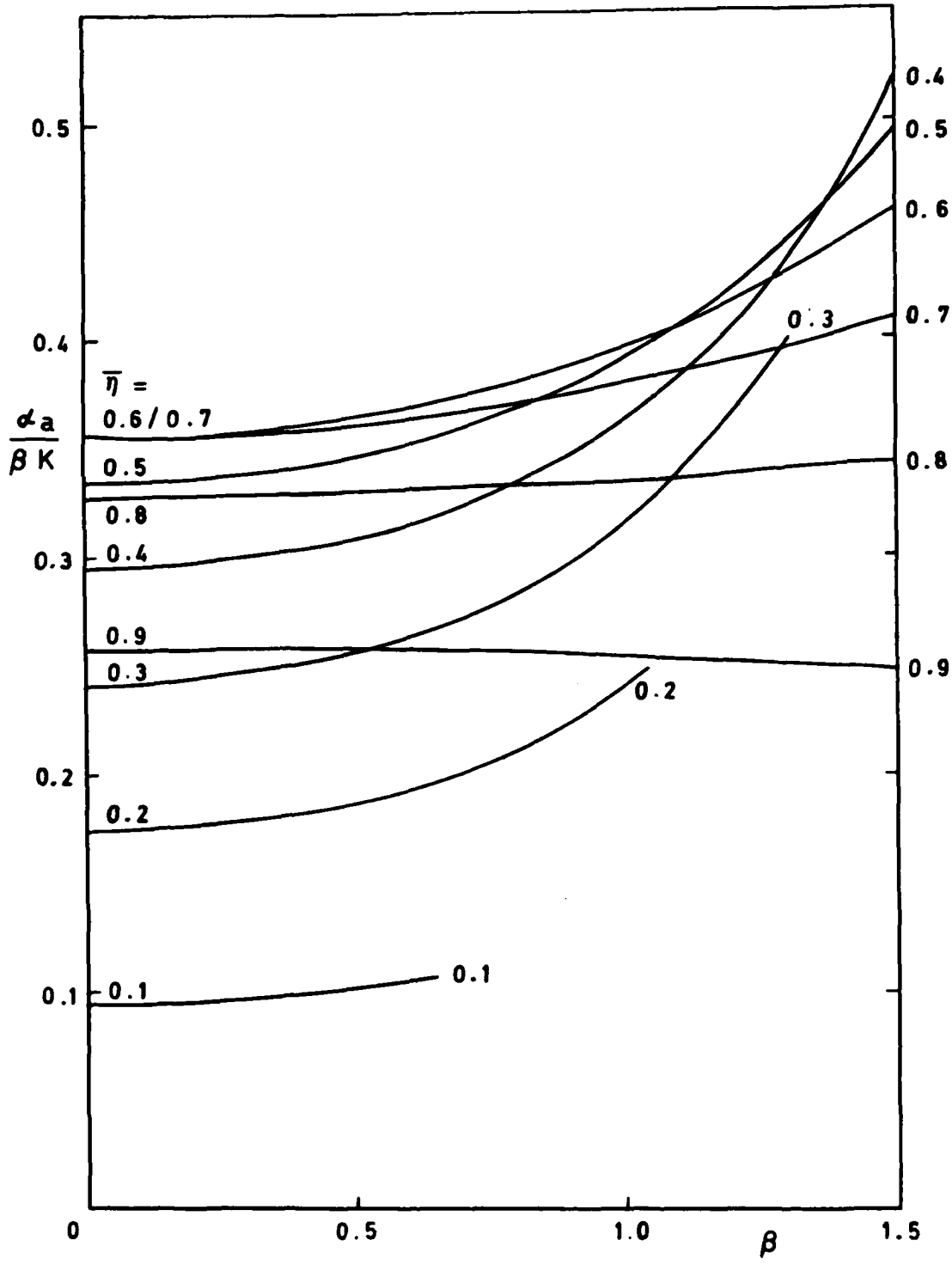

Fig 5 Variation of $\alpha_a/\beta K$ with β for various $\overline{\eta}$

TR 81180

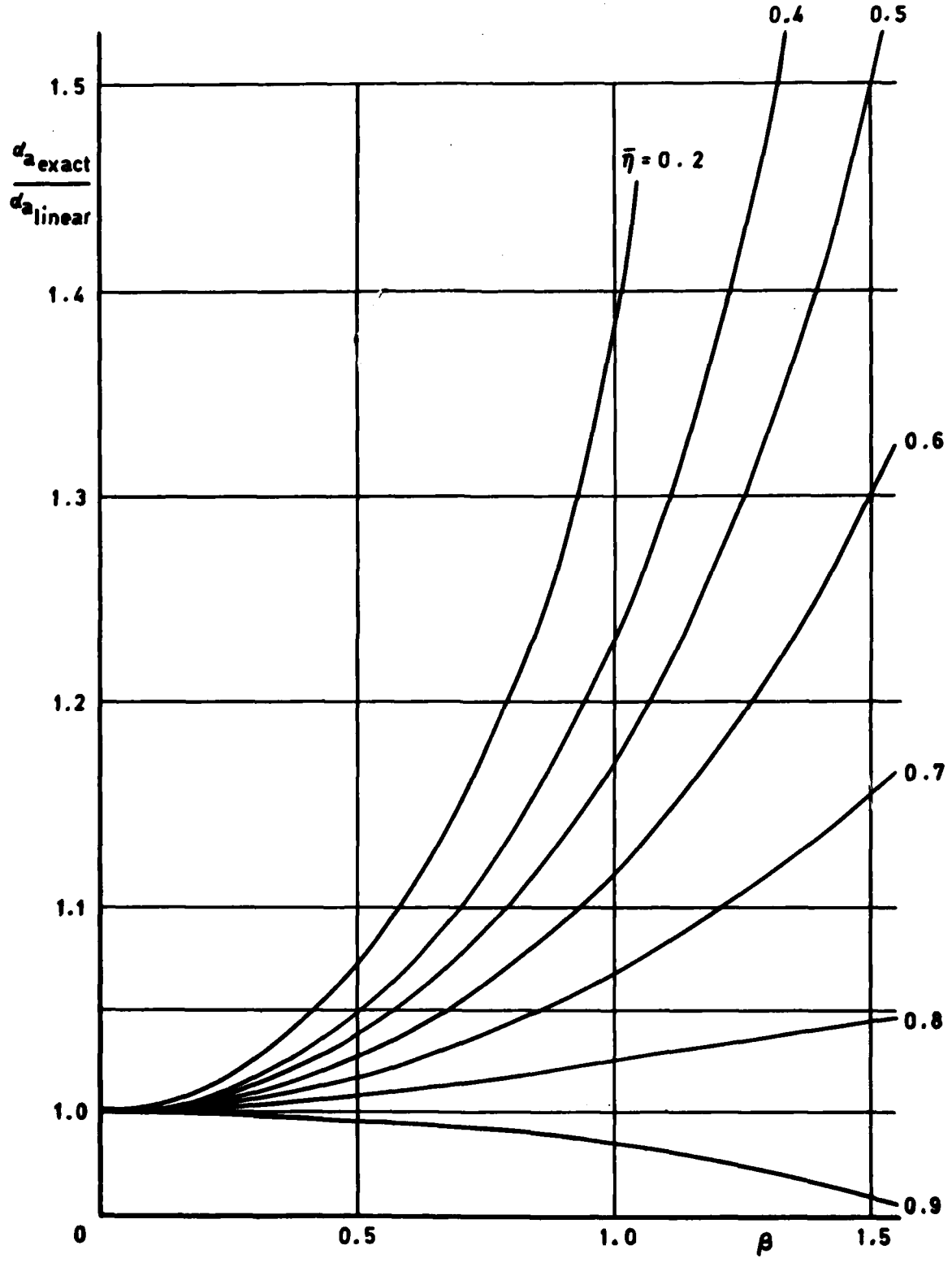

Fig 6 Ratio of 'exact' attachment incidence to its linear estimate for various $\bar{\eta}$

Fig 7

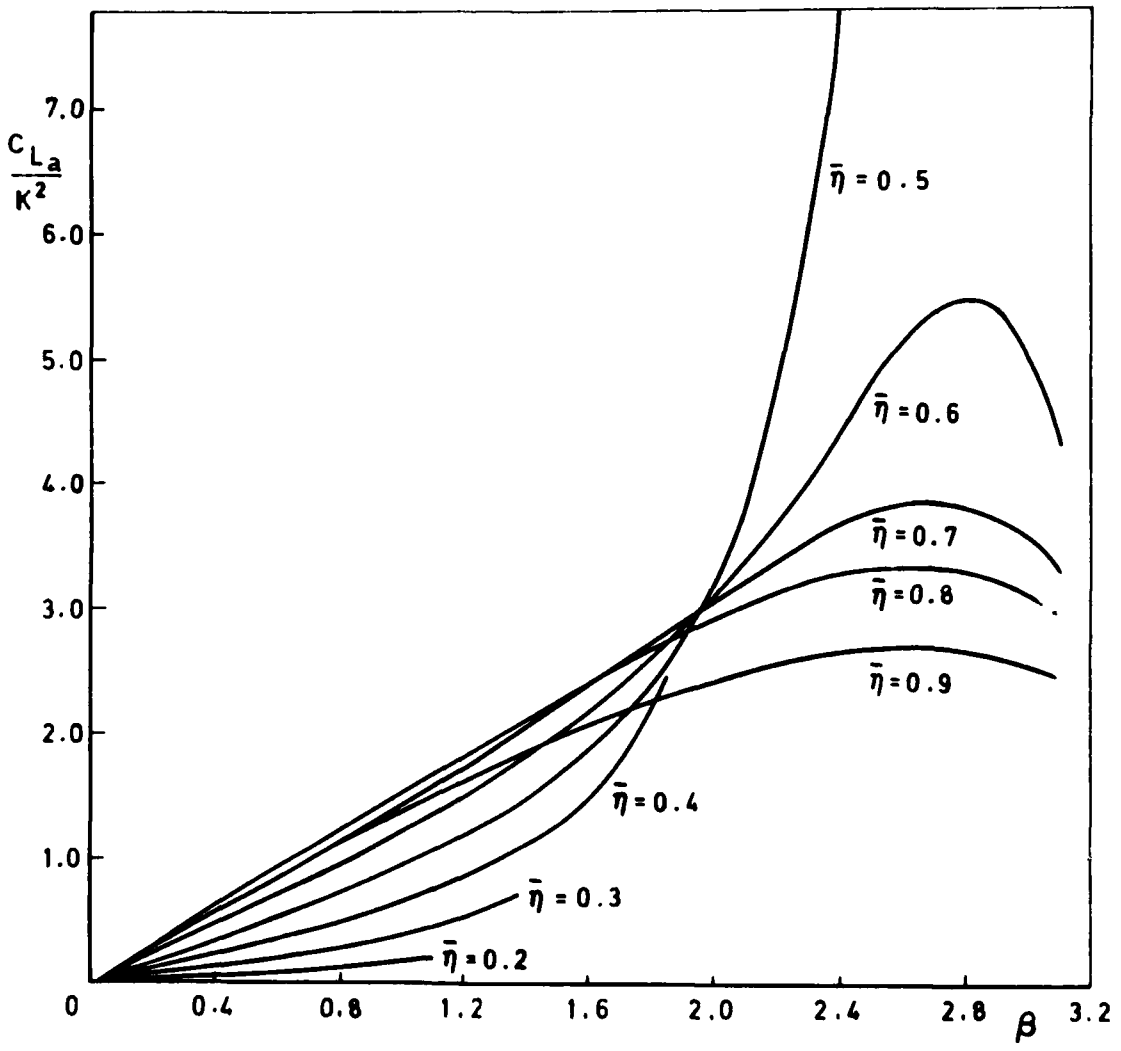

Fig 7 Variation of C_{L_a}/K^2 with β for various $\bar{\eta}$

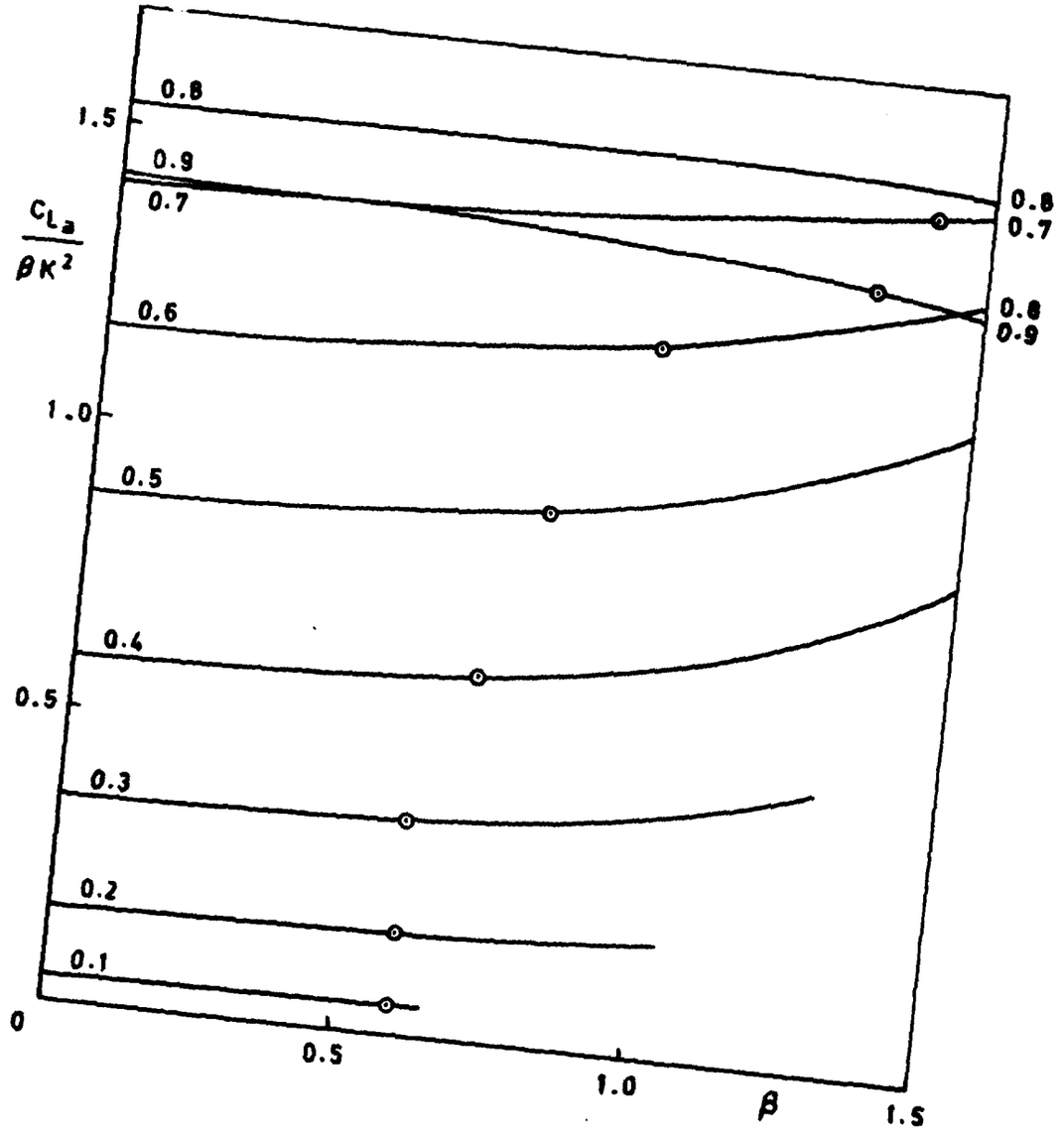

Fig 8 Variation of $C_{L_a}/\beta K^2$ with β for various $\bar{\eta}$

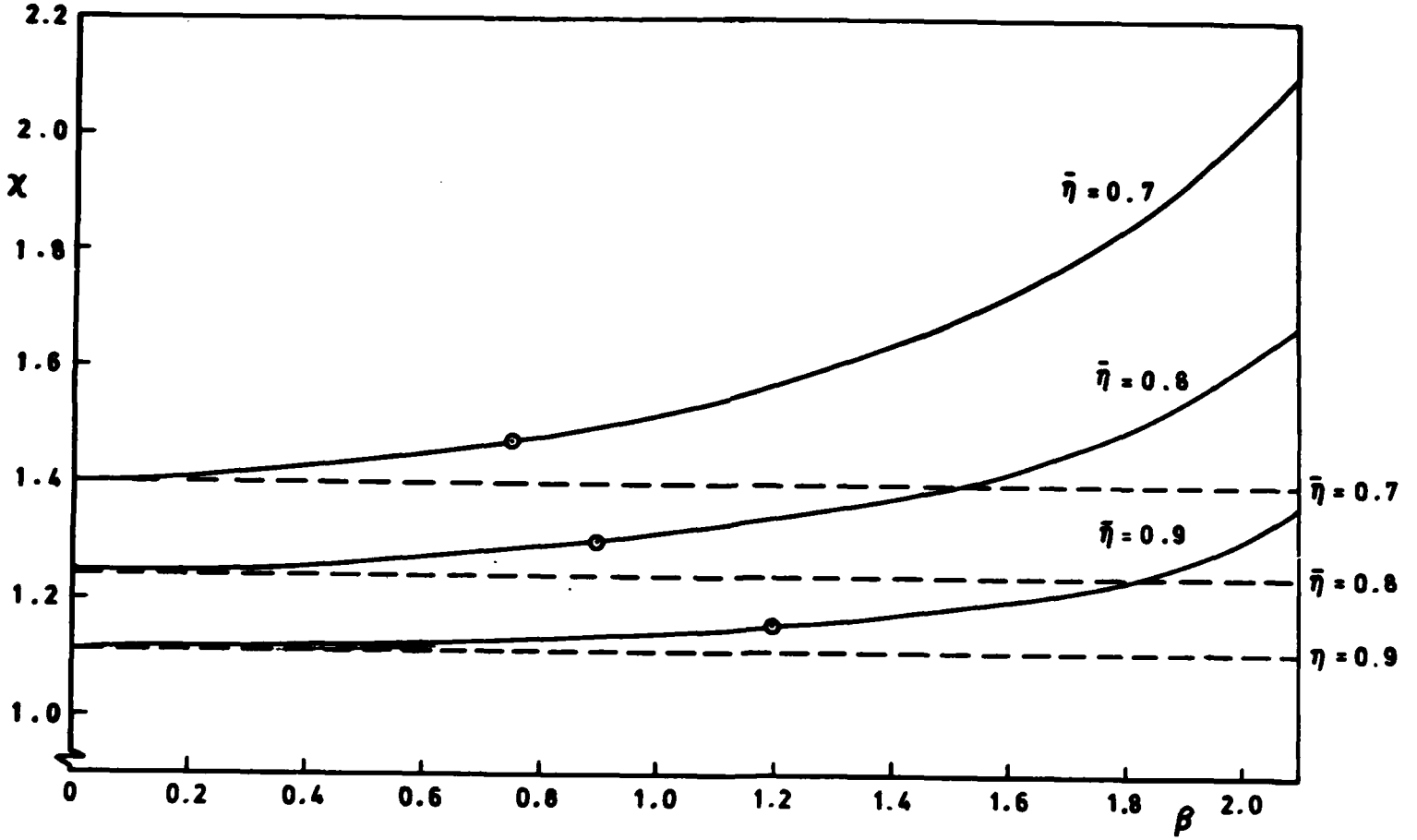

Fig 9 Lift-dependent drag factors at attachment for 'exact' and linearized boundary conditions

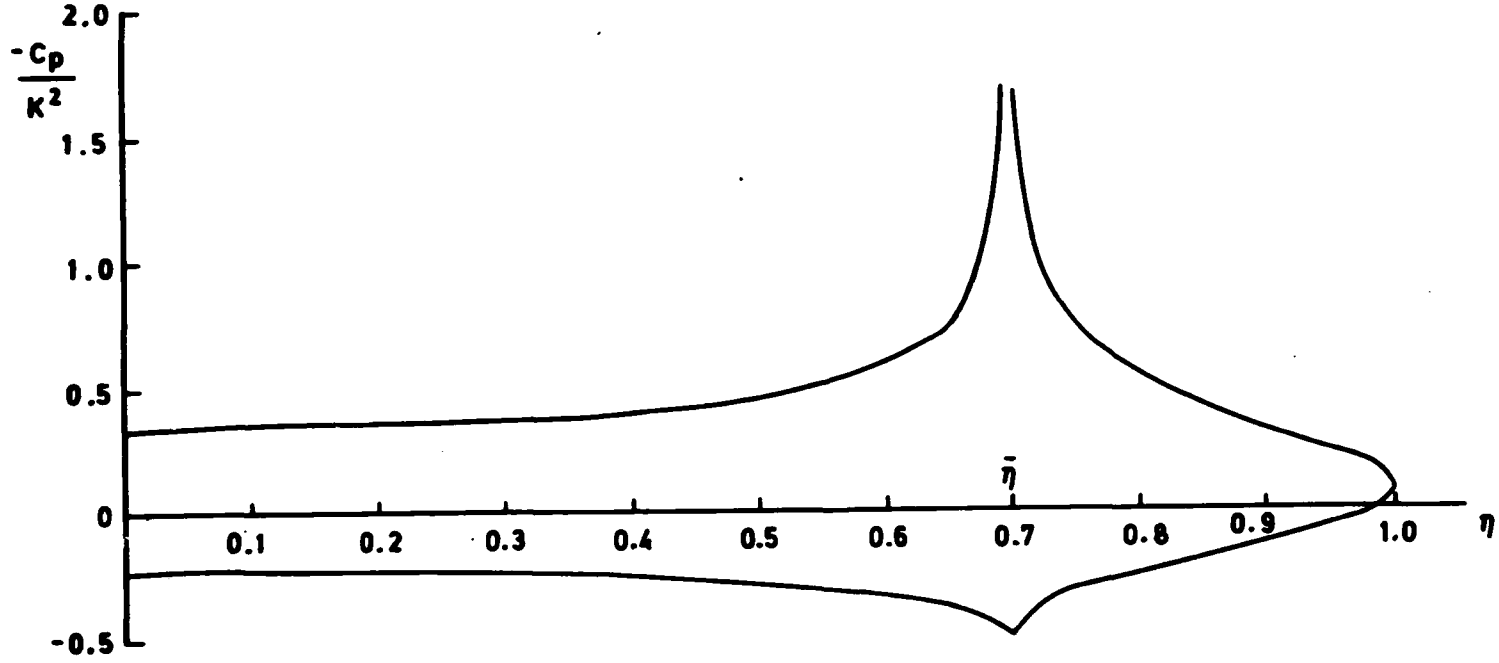

Fig 10 Pressure distribution on wing for $\bar{\eta} = 0.7$, $\beta = 0.5$

Fig 11

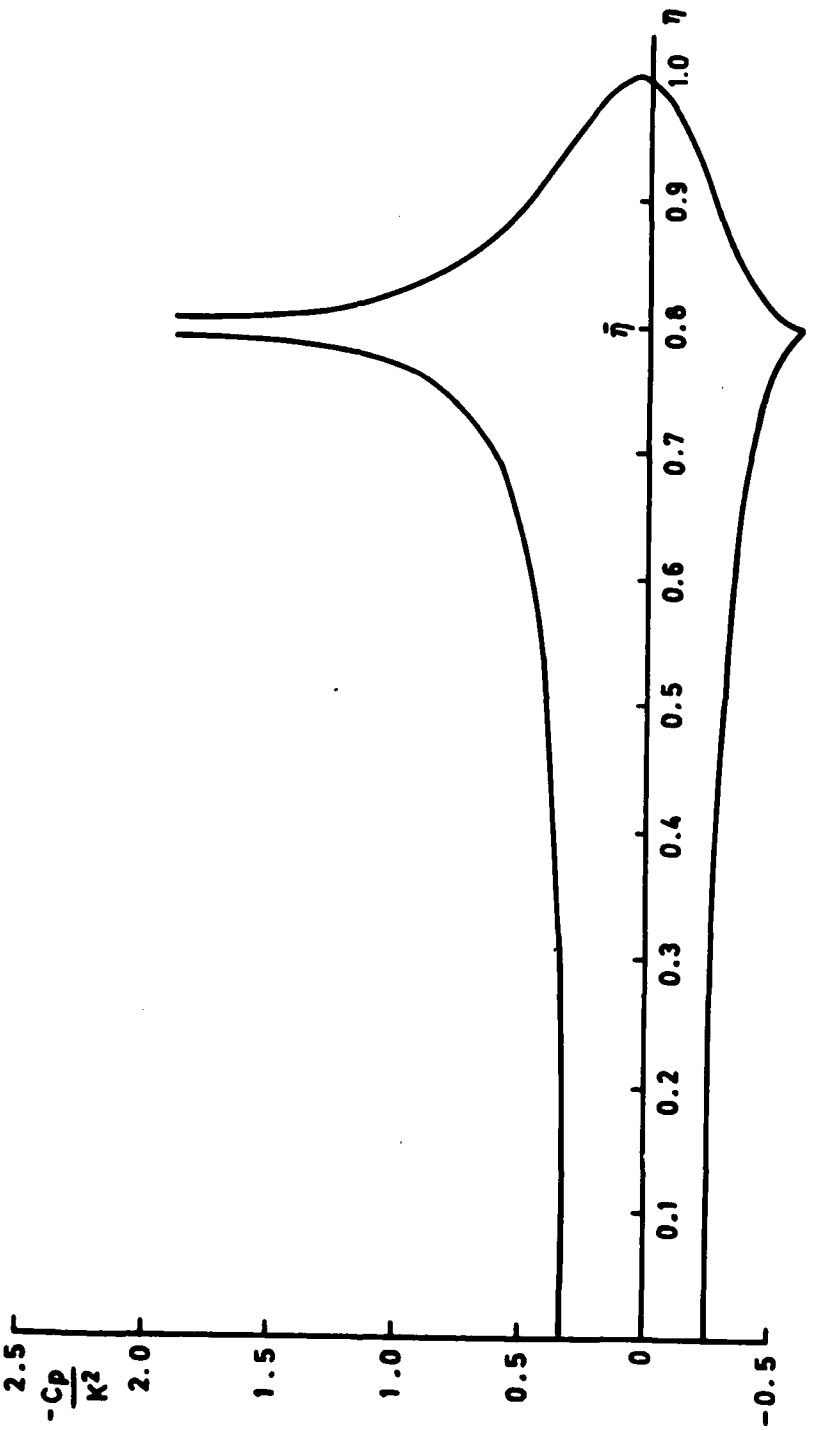

Fig 11 Pressure distribution on wing for $\bar{\eta}$ = 0.8 , β = 0.5

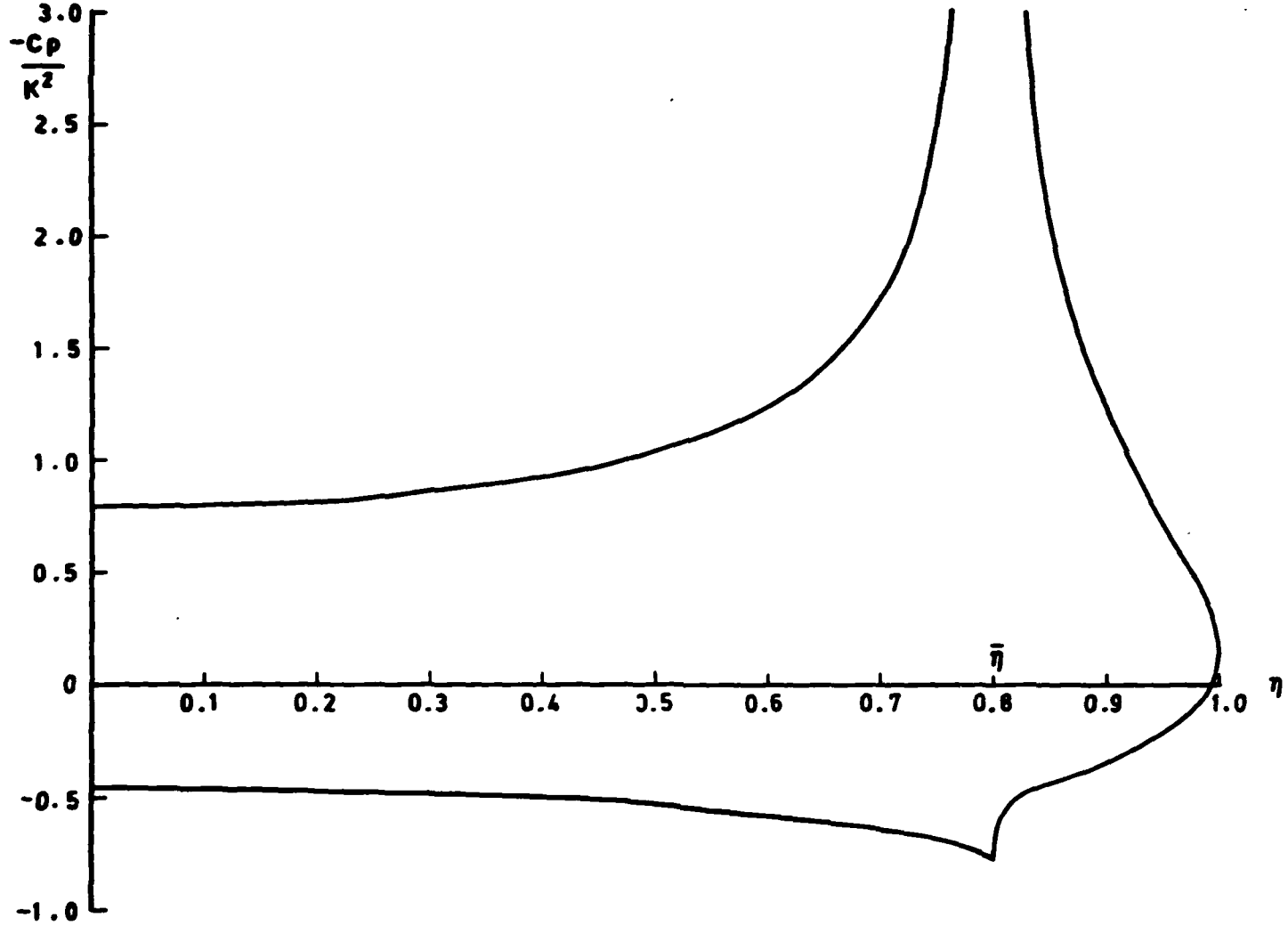

Fig 12 Pressure distribution on wing for $\bar{\eta} \approx 0.8$, $\beta \approx 1.1$

1. [illegible]	2. [illegible]
5. [illegible] Code for [illegible] [illegible]	6. [illegible]
5a. Sponsoring Agency's Code N/A	6a. Sponsoring Agency (Contract Authority) [illegible] [illegible]

7. Title The [illegible] flow over a [illegible]

7a. (For Translations) Title in Foreign Language

7b. (For Conference Papers) Title, Place and Date of Conference

8. Author 1. Surname, Initials [illegible], A.J.	9a. Author 2 –	9b. Authors 3, 4 ... –	[illegible]
11. Contract Number N/A	12. Period N/A	13. Project	[illegible]

15. Distribution statement
(a) [illegible]
(b) [illegible]

16. [illegible]

[illegible]

17. Abstract

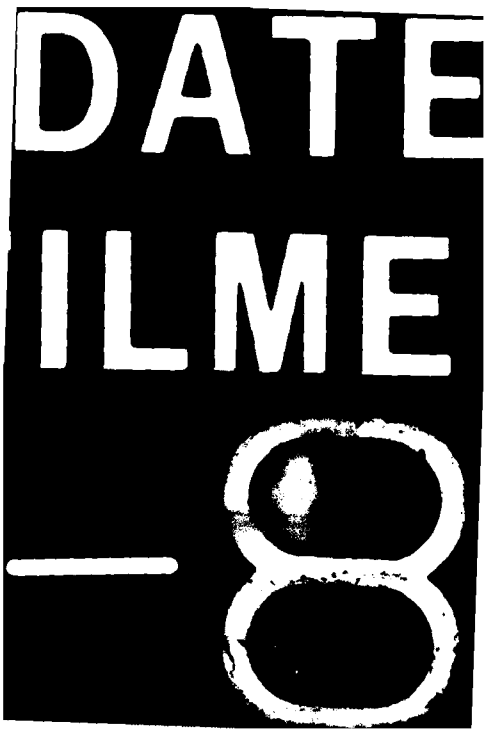
DATE
ILME
8